European Journal of
Biology
(EJB)

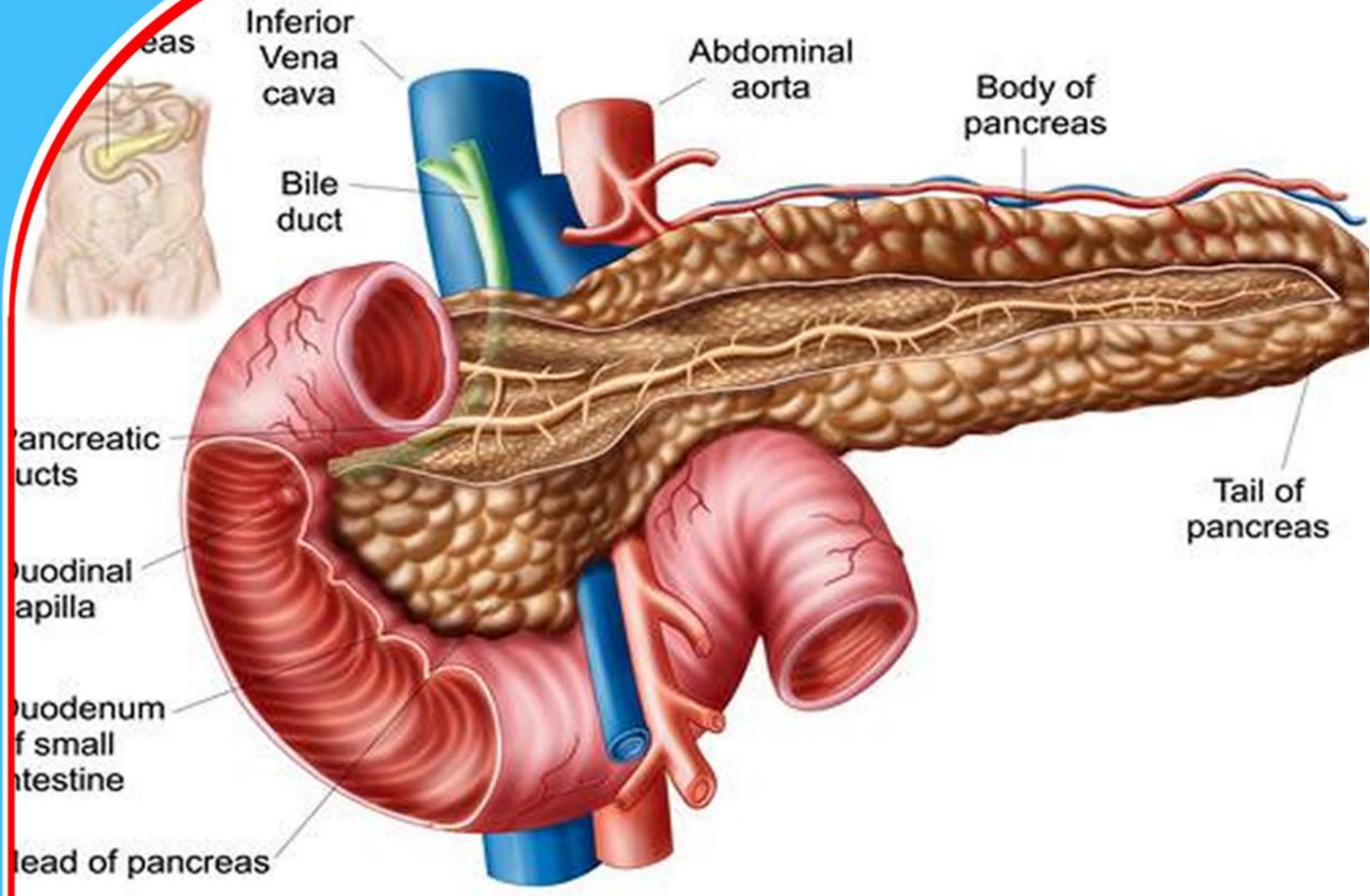

Exploring Proteome of Crimean-Congo Hemorrhagic Fever Virus to Construct Multiepitope Based Subunit Vaccine: Molecular Docking with Immunoinformatic Framework

Hira Shafique, Iqra Shafique, Farah Shahid, Nimra Asif & Usman Ali Ashfaq

AJP

European Journal of Biology
ISSN 2709-5886 (Online)
Vol.8, Issue 1, pp 22 - 43, 2023

www.ajpojournals.org

Exploring Proteome of Crimean-Congo Hemorrhagic Fever Virus to Construct Multiepitope Based Subunit Vaccine: Molecular Docking with Immunoinformatic Framework

Hira Shafique[1*], Iqra Shafique[2], Farah Shahid[3], Nimra Asif[4] & Usman Ali Ashfaq[5]

[*]Corresponding Author's Email: shafiqhira12@gmail.com

Co-Authors Emails: iqrashafique778@gmail.com, farah.shahid.209@gmail.com, nimraasif202@gmail.com & usmancemb@gmail.com

Article History

Submitted 10.10.2023 Revised Version Received 21.10.2023 Accepted 22.10.2023

Abstract

Purpose: Crimean-Congo hemorrhagic fever virus (CCHFV), a single-stranded RNA (ssRNA) virus that spreads via tick bites. For the treatment of CCHFV, there is still a lack of vaccine or any antiviral medicine. For this purpose, a study was performed to design a multiepitope based subunit vaccine (MESV) for effective prevention against CCHFV infection.

Methodology: The study contains immunoinformatic and docking methodologies to obtain a MESV by choosing highly antigenic and overlapping epitopes comprising of 8 epitopes of both MHC class I and II from viral proteins. Epitopes were chosen which were conserved within the epitopes of IFN- gamma, T-cell and B-cell. Then these epitopes were joined to final peptide by GPGPG and AAY linkers. An adjuvant was added at N terminal of vaccine via EAAAK linker for the improvement of vaccine's immunogenicity.

Findings: Our final construct was comprised of 278 amino acids. To validate the vaccine's immunogenicity and safety, its physiochemical properties, allergenicity as well as antigenicity were checked and it was predicted to be non-allergenic and antigenic. The construct was further analyzed by molecular docking within vaccine and TLR3 receptor to assure its molecular interaction and binding affinity. In the end, *In-silico* cloning was also carried out for ensuring its expression efficiency.

Recommendations: Nonetheless, the designed construct is proposed to be tested in laboratory settings to confirm its immunogenicity and safety.

Keywords: CCHF, Immunoinformatics, Bcell Epitope, T Cell Epitope, Subunit Vaccine, Molecular Docking

1.0 INTRODUCTION

CCHFV, a negative-sense ssRNA virus with 100nm in diameter, is placed within Nairovirus genus from Bunyaviridae family (Ergonul, 2012). The viral genome has a length of 19.2 kb, comprising of a 1672 nt small (S) segment, 5364 nt medium (M) section and 12150 nt large (L) section. Small segment participates in the formation of Nucleoprotein, enveloped Glycoprotein (Gc, Gn) are coded by Medium segment and the larger segment encodes RNA-dependent RNA Polymerase (RdRP) (Oany et al., 2015) (Schmaljohn, 2001) (Zivcec et al., 2016) (Zivcec et al., 2018) . In 1994, CCHF was first distinguished in Crimea and named as Crimean-hemorrhagic fever (Whitehouse, 2004) (Casals, 1969).

After certain years, a virus with same pathogenesis was reported in 1956 from an individual in Congo and Africa (Casals, 1969). It was found in the end of 1960s that ingenious agent causing the hemorrhagic sickness in the Crimea have similarity to ingenious agent of the hemorrhagic malady in Belgian Congo and therefore named as CCHF virus (Hawman and Feldmann, 2018). It has a very broad geographic field of the medically important tick-borne virus. On the basis of sequence data, 7 genotypes of CCHFV have been known namely Asia 1, Africa 2, Europe 1, Europe 2, Asia 2, Africa 3 and Africa 1 (Alam et al., 2013) (Mild et al., 2010).

CCHFV is an emerging pathogen whose occurrence as well as geographic range has been expanding from the time of its initial detection. In the recent 20 years, CCHF has risen or reappeared in a few countries regularly with drastically marked up case numbers. Besides this, there has been a notable increase in CCHF cases within South Asian and European countries. The cause of this increased cases is not completely known, however causes, for example, changes in atmosphere, human and animal migrations, population growth in domesticated animals and wildlife along with the changes in farming methods and expanded land-use might be responsible. Hence, there is a need to create therapeutic and prophylactic antidote against this critical rising zoonosis.

In Pakistan CCHFV was early isolated in Lahore in late 1960s (BEGUM et al., 1970). Then it was disseminated in 1976 and since 2010, an increase in the incidence of CCHF has been reported in Rawalpindi and Karachi (Khurshid et al., 2015) (Burney et al., 1980). In first stage of CCHF, the symptoms include vague sickness suddenly. Later on, the infection of CCHFV is characterized by muscle pain, fever, diarrhea, arthralgia, vomiting, bleeding into skin, mood instability, myalgia, urinary tract bleeding, red eyes, photophobia and follow to the liver failure (Emmerich et al., 2018). Before end of second week of sickness, up to 30% of infected people die (Simon et al., 2009).

CCHFV usually transmits by tick bites or with pets that carry disease of *Hyalomma* genus, despite the fact that there is limited proof that different types of ticks, for example, Ornithodoros, Rhipicephalus, Ixodes, and Dermacentor may likewise be vectors (Bente et al., 2013) (Saleem et al., 2016) . The Hyalomma vector have been discovered all over Africa, Southern Europe, Middle-East, Asia, Eastern Europe countries and CCHF have also been reported in these areas. A predicted 10k to 15k CCHFV human infections arise annually, even though most of these are without symptoms and unrecognized (Ergönül, 2006). The individuals who get infected are usually farmers or laborer in slaughterhouse. At the point when bunches of disease happen, it is regularly after individuals treat, butcher or eat contaminated domesticated animals, especially ruminants and ostriches.

Humans contaminate humans as well as breakouts additionally happen in clinical offices by taint blood and impure medicinal gadgets. Review considers in people have recognized links among polymorphisms between Toll-like receptors (TLRs) and harshness of illness, proposing that Toll-like receptors might be significant and are resistant against CCHFV. Unfortunately, up to this point there is no authorized vaccine or endorsed focused on treatments and prevention of CCHF, despite the fact that Ribavirin can assist a great deal with treating the disease (Dowall et al., 2017) (Keshtkar-Jahromi et al., 2011) (Yilmaz et al., 2009).

Bioinformatics as well as other computational tools can give huge immunological information, for example, antigen processing and presentation, antigen assurance as well as antigen-antibody interactions to acquire expressive elucidations. In this way, nowadays process of designing vaccine particularly MESV development is made possible with bioinformatics tools, for example, protein modeling software, epitope mapping (programming/web administration) and protein-protein/ligand interaction analysis software (Soria-Guerra et al., 2015). With ongoing progress in bioinformatics, MESV has become another way of predicting the potential epitopes and acquiring humoral (B-cell) as well as cell-mediated (CTL &HTL) immunity (Davies and Flower, 2007).

In this study, proteins of CCHFV were chosen for predicting the epitopes of IFN- gamma, T cell and B cell. Conservational analysis was done and highly conserved, antigenic and overlapped epitopes were separated and integrated through adjuvants and linkers to compose MESV. GPGPG linkers in MESV maintains a strategic distance from cohort of coupling epitopes, that is considered a significant concern for structure of vaccine moreover, it encourages immunization of helper T-lymphocyte epitopes while adjuvants are used to increase immunity to vaccine (Coffman et al., 2010). Physiochemical properties, antigenicity as well as structural attributes were examined using various online tools. Moreover, docking analysis was carried out between vaccine and TLR3. *In-silico* cloning was also done for testing the progressed polyprotein arrangement.

2.0 METHODOLOGY

Sequence Retrieval

In initial step, CCHFV proteins sequences which includes Glycoprotein, Nucleoprotein and RNA Dependent RNA Polymerase were fetched in FASTA format from Genbank (Benson et al., 2008).

Conservation Analysis

Using ClustalW, multiple sequence alignment (MSA) was carried out for identifying the conserved regions within protein sequence of all CCHFV genotypes. BioEdit tool was utilized for visualizing the consensus regions created from all genotypes (Hall, 1999; Li, 2003).

Prediction of *T-cell* Epitopes

MHC class I epitopes

NetMHC 3.4 server was utilized for the prediction of the binding of peptide sequences to various HLA class I alleles thorough Artificial Neural Networks. The affinity of every protein was tested for binding with HLA A and HLA B with A*0101, B*0702, A*0201, A*2402, A*0301, A*2601, B*0801, B*3901, B*2705, B*4001, B*1501, B*5801, as agent alleles. Peptide length was fixed to 12mers as it is a length bound easily by class I alleles and ANNs have likewise been prepared on 12 mer peptides. From this examination, strong binders were deduced, keeping threshold to less than 50nM (Lundegaard et al., 2008).

MHC Class II Epitopes

Immune epitope database-Analysis Resource (IEDB-AR) was utilized for predicting the 15-mer T-cell epitopes for human alleles like HLA-DRB1*01:01, HLA-DQA1*01:01/DQB1*04:02, HLA-DPA1*01:03/DPB1*05:01, HLA-DRB1*09:01, HLA-DPA1*01:03/DPB1*14:01, HLA-DRB3*02:02, HLA-DPA1*01:03/DPB1*01:01, HLA-DRB1*11:01 and HLA-DRB1*04:01. The peptides have been categorized as strong, weak and non-binders. The threshold values for strong, weak and non-binder were set as 2%, 10% and more than 10% correspondingly (Wang et al., 2010).

B Cell Epitope Prediction

To identify the B-cell epitopes for proteins of CCHFV, an online server ABCPred was used by setting the threshold value at 0.51(Saha and Raghava, 2006).

Immunogenic Peptide Prediction

To analyze the antigenic reactivity of B cell as well as T cell epitopes, Vaxijen 2.0 tool was operated by keeping the threshold value at 4.0 correspondingly (Doytchinova and Flower, 2007). Antigenic epitopes were screened out for more study and non-antigenic epitopes were excluded.

Interferon-Gamma Inducing Epitope Prediction

IFN-gamma induces immune response and is involved in direct inhibition of viral replication. Furthermore, they can produce immunological reactions by activating the cytotoxic and helper T cells. IFNepitope web server predicts the IFN-gamma epitopes of chosen CCHFV proteins utilizing SVM based Motif and hybrid algorithms (Dhanda et al., 2013).

Multi-epitope vaccine construction:

The selected MHC I and II epitopes from 2 CCHFV proteins were joined to form the vaccine construct. These epitopes must be immunogenic, overlapping and preserved. Adjuvant was also joined to N-end of vaccine. The CTL epitope and adjuvant were merged through EAAAK peptide linker, while GPGPG and AAY linkers were utilized for joining the other epitopes of MHC I and II correspondingly.

Linear and Conformational B Epitopes and Physiochemical Properties Assessment

ProtParam tool was employed for the determination of physicochemical characteristics of multiepitope vaccine. It reviews distinctive physicochemical traits which are reliant on pK approximations of amino acids included. Confinements to which polyprotein sequences were subjected are Instability Index, Aliphatic list, Grand Average of Hydropathicity, Hypothetical pI, Stability profile and half-life (Gasteiger et al., 2003). Linear B-cell epitopes (14-mer) of final vaccine construct was identified through ABCpred. Discontinuous (conformational) epitopes were predicted with DiscoTope 2.0 server. Location of the epitopes on 3-dimensional structure of vaccine was examined through Pymol (DeLano, 2002).

Antigenicity and Allergenicity Prediction

Allergic and non-allergic nature of vaccine was assessed through AllerTOP V2.0 server. It symbolizes the info protein sequence by applying k-nearest neighbor estimation (kNN; k = 3) based on direction set having predominant 2210 non-allergens from same species and 2210 allergens from distinct species (Dimitrov et al., 2013). Vaxijen server was utilized to identify the

antigenicity of vaccine which depends on various physicochemical characteristics of protein and is alignment-free in Vaxijen.

Prediction of Secondary Structure

SOPMA was utilized to predict secondary structure of vaccine. Degree of beta-turn, alpha helices, arbitrary loops and extended strand was surveyed with the help of this software. The outcomes demonstrated two graphs from which one portraying the prediction while the subsequent demonstrating score curves for predicted positions. Further, it shows the requirements, for instance, window width, various states etc. that is utilized for prediction (Deléage, 2017).

Prediction of Tertiary Structure

RaptorX web server was utilized for predicting the 3D structure of the final multiepitope vaccine (Peng and Xu, 2011). The prediction through RaptorX is based on features like assessment of alignment quality, single template based threading and multiple template based threading. This tool utilizes the template for structure modeling thereby generating the high quality aligned structure (Peng and Xu, 2011). Mod refiner and GalaxyRefine server were utilized to refine the tertiary structure of the vaccine anticipated by Raptor x. ModRefiner created refined full-particle models from Ca trail with better worldwide and different attributes (Xu and Zhang, 2011). Galaxy refines utilized strong and delicate unwinding strategy for refining the structure of the protein. It produces numerous models with structure deviancies from the given structure. After that, the Ramachandran plot generated by a server RAMPAGE was employed for validating the tertiary structure. The outcomes of RAMPAGE finishes up the quality of retrieved structure that involves a portion of residues present in exception along with permitted regions(Lovell et al., 2003). The analysis by PROSA program was further carried out for authentication of protein structure. This also involves the assessment of the predicted structure with the quality score. However, if the local protein score reaches beyond the defined limit, it was considered a false score for structure (Wiederstein and Sippl, 2007).

Disulfide Engineering for Improved Vaccine Stability

Prior to continuing to the subsequent stage, stability of the predicted protein model should be improved. Disulfide (S-S) bonds are the covalent interactions to give significant stability to a protein model by verifying exact geometric compliances. It is an innovative methodology for making S-S bonds into objective protein structure. Hence, the refined model of final vaccine was then subjected to Disulfide by Design 2.0 (DbD2) to perform disulfide engineering (Craig and Dombkowski, 2013). At first, residue pair was searched that can be utilized for the disulfide building approach by taking refined protein model as an input. Absolute 2 residue sets were chosen to change them with the residue of cysteine by utilizing the create, mutate column option in DbD2 server.

Molecular Docking of Immune Receptor (TLR3) with Vaccine Candidate

For suitable elicitation of immune response, the presence of interaction among the immunologic receptor as well as the antigen is quite important. Molecular docking was done for analyzing the interaction among ligand (vaccine) and immunologic receptors (TLR3). To validate the immune responses, the vaccine construct was docked with the TLR-3 using the GRAMM-X that employs knowledge-based scoring, refinement stage and smoothed potentials (Tovchigrechko and Vakser,

2006). Interacting residues of docked complexes were denoted by database PDBsum (Laskowski, 2009).

Molecular Dynamics Simulation

The study of molecular dynamics (MD) is necessary for investigating strength of protein complex in the insilico study. To clarify the aggregate protein movement in the inward correlates through normal mode analysis (NMA), iMODS server was utilized. The server evaluated the course and degree of the inborn movements of complex regarding eigenvalues, covariance, B-variables and deformability. The deformability of leading chain relies upon whether a predetermined molecule can misshape with its each residue. The Eigenvalue portrays the unbending nature of movement. The value is connected legitimately to energy needed for the structural deformation as well as low eigenvalue is essential for deformation.

Vaccine Immunogenicity Assessment

Insilico immune simulation was performed through C-ImmSim 10.1 server to validate the immunological responses of the designed MESV. C-ImmSim simulates the three main components of the functional mammal system (Thymus, lymph node, and bone marrow) (Rapin et al., 2010). The parameters for the simulations were: volume (10), HLA (A0101, A0101, B0702, B0702, DRB1_0101, DRB1_0101), random seed (12345), no. of steps (100), no. of injection (1). The rest of the parameters were considered to be the default.

In-Silico Cloning

Reverse translation and Codon optimization were assessed through codon adaptation tool for validating the expression in vector and translational efficiency of the cloning. *E. coli* (K-12 strain) was selected as a host for determining the expression of predicted vaccine construct. The other available choices were selected to evade: (i) termination of intrinsic transcription, (ii) binding-site of prokaryote ribosome, and (iii) cleavage-sites of restrictase/restriction endonuleases. Codon adaptation index (CAI) (Sharp and Li, 1987) along with the GC (guanine and cytosine) contents were assessed. Sticky ends of the restriction sites of BamHI and HindIII were introduced to allow restriction and cloning, correspondingly. The modified nucleotide sequence of MESV was additionally cloned within *E. coli* pET30a (+) vector using SnapGene tool, to assure its *in-vitro* expression.

3.0 FINDINGS

Conserved Sequences of CCHFV Proteins

The investigation of conserved regions is broadly utilized for identifying the functionally important residues within protein sequences. There are 3 proteins for CCHFV i.e. Nucleoprotein, Glycoprotein and Rdrp from which nucleoprotein found to be non-antigenic and other 2 were found antigenic and those were selected for further analysis. The conserved regions among the chosen structural and nonstructural protein of all genotypes are shown in (Table 1) which are 2 for Rdrp and 15 for Glycoprotein. Utilizing this analysis, these sequences were also chosen for T cell, B cell, and IFN-gamma epitope prediction.

Epitope Prediction

Total 24 MHC class I (9 RdRP and 15 Glycoprotein) (Table 2), 27 MHC class II (14 RdRP and 13 Glycoprotein) (Table 3) and 31 linear B-cell epitopes (8 RdRP and 22 Glycoprotein) were

picked out (Table 4). After that, these were further assessed according to their high scores as well as binding affinity to the vast majority of alleles related with CCHFV clearance or protection. Additionally, for each viral protein, prediction of epitopes for T-cell, B-cell and IFN-gamma was done. At last, the T-cell epitopes which were common to the identified B-cell and IFN-gamma epitopes were chosen. Moreover, these epitopes were also assessed through BLASTp to avoid homology with the host proteins. The validated epitopes were then evaluated for their antigenic reactivity and strong antigenic epitopes were further examined.

Multiepitope Vaccine Construct

The epitopes shortlisted for analysis harbors following properties: T-cells showing high-score and strongly binding to a number of alleles, also, sequences should be overlapped with the epitopes of B cell and IFN-gamma, needs to be non-homologous to human and strongly antigenic. In light of previously mentioned criteria, just 16 epitopes were chosen. Among shortlisted epitopes, 8 were available in MHC class I from which 7 were found in Rdrp and 1 epitope was found in Glycoprotein while 8 were available in MHC class II in which 5 epitopes were found in Rdrp and 3 were available in Glycoprotein (Table 2). For designing multiepitope based vaccine construct, 16 epitopes were selected and consolidated with the assistance of an adaptable linker i.e. AAY. The construct of final vaccine was found consisting of 233 amino acids. Additionally, an adjuvant named beta-defensing, 45 long chain amino acid was introduced with EAAAK linker at N-terminal. The final length of construct was then increased to 278 amino acid after joining of adjuvant and linkers (Figure 1).

Conformational and Linear B Epitopes and Physiochemical Characteristics of Vaccine Construct

Allergenicity and antigenicity of the vaccine was assessed through AllerTOP V2 and Vaxijen server respectively. The outcomes showed that vaccine candidate was non-allergenic and antigenic. Antigenicity value of vaccine was calculated as 0.6779. Different physiochemical features of vaccine candidate were identified through ProtParam tool. The PI of construct was 8.58, representing it as basic and its molecular weight was 29348.78 kDa. The aliphatic index is 86.62 portraying it as thermostable. The predicted half-life of the vaccine construct was calculated as almost 30 hours invitro (mammalian reticulocytes) and >10 hours and >20 hours in-vivo (E. coli) respectively. GRAVY was found to be 0.037, the value in positive sign indicates its hydrophobic nature. By utilizing ABCpred and DiscoTope 2.0 server, twenty-two continuous B-cell epitopes were recognized within the vaccine construct. Pymol was employed for visualizing the epitopes location on 3D vaccine structure Figure 3.

Secondary Structure Prediction

To predict secondary structure, an online SOPMA server has been utilized which determines the features of secondary structure depending upon the primary sequence of the protein. Within 278 amino acids, 137 were involved in constructing alpha-helix that represents 49.28% of the construct, 43 in beta-(15.47%), and protein coils were constructed by 89 amino acids (32.01%).

Tertiary Structure Prediction and Refinement

RaptorX is a tool reachable on web to foresee and examine structure of protein. It was utilized for portraying tertiary structure arrangement of designed vaccine. Input was given in the form of amino acid sequence which contain four domains, while 1kj6A model was utilized as a template.

The calculated P-value of the modeled protein structure was relatively low i-e 2.18e-08, showing the model's higher quality. All 278 amino acids were modeled, only 45 (16%) positions were identified as disordered within the model. The vaccine 3D structure was improved by utilizing mod refiner in addition to Galaxy Refine server. After refinement, it produced 5 models. After conforming scores of these 5 models, model 5 was seen as best model, so that was picked.

The model exhibited 96.7% favored region within the RAMPAGE and showed poor rotamers: 1.0, qRMSD: 0.423, MolProbity: 1.816, clash score: 12.5 and RAMPAGE evaluates as well as verifies 3D structure through Ramachandran plot. As indicated by this plot, 97.1% of residues exist in favored region, 2.9% resides within allowed region as well as 0% is shown in outliner regions. Moreover, ProSA-web calculates −5.07 Z score that wins inside extent of commendable scores. What's more, the refined model indicated 3 errors with PROCHECK. The refined model was 90.583 in absolute quality (ERRAT score). These outcomes revealed that our refined vaccine model is of acceptable quality (Figure 2).

Disulfide Engineering for Vaccine Stability

Disulfide engineering was carried out utilizing the Disulfide by structure v2.0 for stabilizing the modeled structure of the final constructs and absolute 22 sets of residues were found that can potentially be utilized for disulfide engineering. However, upon assessment of different parameters such as Chi3 value as well as energy, just four sets of residues were selected on the grounds that their values goes under the permitted extend for example energy value was under 2.2 and Chi3 was in the middle of −87 to +97 degree. Therefore, absolute 4 mutations were made at the residue pairs in particular Gl116-Tyr122 and Glu173-Ala183 (Figure 4).

Molecular Docking

Immune response activation needs proper interaction among immunologic receptor and antigenic molecule. For docking of construct with TLR-3, GRAMMX tool was applied. In docked compound, TLR3 was depicted in purple color, and the construct in red color, correspondingly, (Fig. 5A). Additionally, an online server PDBsum was employed to accomplish the ordinary sketch of collaboration between docked-complex. It delivered graphic depiction of hydrogen-bond and nonbonded collaborations between docked proteins-complex. It was seen that MESV makes one hydrogen bond with TLR3 (Fig.5B).

Molecular Dynamics Simulation

NMA was employed for investigating the protein adjustment and their wide-ranging flexibility. This assessment was carried out through iMODS server on the basis of inner directions of docked complex. The deformability of complex relies upon the individual twist of every residue, delineated by the chain pivots (Fig. 6b). The eigenvalue revealed to be 4.372843e−07 (Fig. 6a). The change connected with every mode was reversed with the eigenvalue. The B-factor esteems produced from the mode examination were relative to the RMS (Fig. 6c). Covariance lattice appearing different sets of related, un-correlated and anti-correlated movements were showed by red, white as well as blue colors (Fig. 6d). The outcome additionally gave a versatile model that recognized the sets of molecules connected through various springs (Fig. 6e). Each spot within the chart giving one spring, shaded with the degree of firmness, in the relating atom sets. More dark grays shows more unbending of springs.

Immunogenicity Evaluation of MESV

The *in-silco* host immunological response against the antigen is exhibited in Figure 7. The primary response was characterized by high IgG + IgG and IgM concentration, followed by IgM, IgG1 and IgG1 + IgG2 at both the secondary as well as primary stages with the associated antigen reduction. Furthermore, robust interleukin and cytokine response was examined. All of this indicates the pathogen's successful immune response as well as clearance after subsequent encounters. In response to the antigen, higher population of B cell including the memory cells and various isotypes contributes in long-lasting memory formation and isotype switching. Besides cytotoxic T cell, the T helper cell population and their respective memory cell are firmly in accordance with a positive antigen response.

***In-silico* Cloning**

Codon adaptation server was exploited for creating cDNA sequence pursued by evaluation of codon optimization that assesses the GC content and CAI. GC content of construct was measured as 57.3% which remains within perfect rank (30% to 70%), yielded codon adaptation index as 0.8 that likewise resides in worth (0.8 to 1) that portray huge protein expression, enhancing the protein reliability. In the following step, both ends of MESV optimized nucleotide sequence were attached to buffer compatible restriction endonucleases BamHI and HindIII restriction sites for carrying out purification/cloning process. Finally, the refined MESV sequence was cloned to the several cloning sites of the pET30a (+) vector between the restriction sites BamHI and HindIII. The clone was 6.23 kbp long (Figure 8).

Discussions

Vaccination is taken as to be most effective process for prevention of infectious diseases. Vaccines act by animating the immune system. A healthy person's immune system can consider attacking microbes as well as infections and generate antibodies to kill them. Vaccinations set up the immune system to avert an infection. To produce immunity to counter viral disease, the killed or weakened virus is used in the vaccine. Vaccines are now generally viewed as a successful and modest tool for improving health. Against major diseases, children are being vaccinated worldwide, and the training has become a focal board of worldwide public health endeavors. Regardless of these advances, in any case, vaccination inclusion stays a long way from general and the evolving world specifically stays in danger to vaccine-curable diseases (Patronov and Doytchinova, 2013). Subunit vaccines utilize just the antigenic parts which best animate immune system, rather than dealing with entire microbe. Subunit vaccine acquaints one antigen to immune system excluding all viral particles (Dodds).

Immunoinformatic methodologies utilizes the computational and mathematical ways to comprehend, produce, process, and develop immunological information. Immunoinformatics look into stresses for the design and investigation of formulas for aligning the epitopes for T cell and B cell that accelerates the time as well as brings down cost required for the research of microbe gene yield. Since the 1980s, different immunoinformatic tools were developed and utilized focusing on vaccine design and it is starting to set up itself as an essential tool within vaccine revelation (Dodds) (Tomar and De, 2010).

The purpose behind the study is to design MESV for raising safety measures against CCHFV. MESV vaccine is favorable upon monovalent vaccine while it can inspire humoral as well as

cellular immunities. As of late; a few endeavors have made for presenting a new vaccine to cure the infection. For this purpose, a peptide vaccine was developed but that study includes only one protein (Tipu, 2016) but this study included 2 proteins and more numbers of epitopes. So, this prevailing vaccine is farther effective as well as immunogenic to counter CCHFV.

Two targeted proteins, RNA dependent RNA polymerase and Glycoprotein were selected and their conservational analysis was done. For designing a vaccine, identification of the T cell as well as the B cell epitopes was the first primary step and then overlapped B-cell & IFN-gamma epitopes have selected and analyzed to predict antigenicity. To develop vaccine, the chosen epitopes have arranged with the assistance of GPGPG and AAY linkers and adjuvant at N terminal of the vaccine. Adjuvant enhances production of antibody and aides in giving hard-core defense.

After joining of adjuvant and linkers, final vaccine construct was seen as 278 amino acid long. The PI of construct was 8.58, depicting it as basic and its molecular weight was 29348.78 kDa. On the basis of theoretical pI value, MESV was found to be basic that can guarantee strong physiological pH interaction. Calculated scores of aliphatic and in-stability index showed that the vaccine construct is stable and thermostable. Hydropathy value recommends its hydrophobic nature. MESV was seen as profoundly antigenic, non-allergenic and immunogenic demonstrating an epitope vaccine's capability to cause hearty immune reactions with no allergic reactions.

Study of the physiochemical characteristics of vaccine construct described it as fundamental, hydrophobic, basic and stable in nature. Moreover, the stability of the final model was approved by Ramachandran plot. To evaluate enough binding for stimulating immunological response, the construct created was docked against the TLR3. It has been suggested that TLR-3 raise the immune system at the time of infection, thereby contributing in active surveillance of the infectious cells.

Epitopes of B and T cell containing MESV should hypothetically activate both humoral and cellular immune reactions. With substantial IL-10 and IL-2 activities, our vaccine demonstrated the highest production of IFN-ÿ. Antibodies also provide extracellular SARS-CoV-2 protection. We have also noticed excess immunoglobulins that are active, i.e., IgM, IgG, along with their isotypes that might be involved in switching isotype. The translation regulation of foreign genes inside the host varies because of the inconsistency of mRNA codons, which need codon optimization for excessive expression (Pandey et al., 2018). CAI value got was 0.8 and GC content (57.3%) was additionally inside the appropriate limit inside E.coli K-12 framework. The main aim of MESV in silico cloning was to direct genetic engineers and molecular biologists on the expected expression level and the potential cloning sites in a particular expression system i-e E. coli K12 system.

Hence, multi-epitope vaccine structured with care utilizing such a technique could turn into an essential resource in the fight against tumors and viral diseases. The findings of current research recommend that designed vaccine should undergo in vivo as well as in vitro test investigation for designing a potent vaccine for CCHFV infection.

4.0 CONCLUSION AND RECOMMENDATIONS

CCHFV is now emerging as an open issue of global interest. However, for this disease, no vaccine or chronic treatment is available yet. A few antiviral drugs have experienced preliminaries, yet none showed viable outcomes to counter the infection. In present study, an attempt was made to find a multi-epitope-based vaccine for CCHFV consolidating on the nonstructural and structural

proteins of infection. Immunoinformatic along with several tools of docking were used for formulating an effective and safe multi-epitope vaccine which may provoke immune responses to be specific innate, cellular and humoral immunological responses. Activation of such immune reactions may control the infection of disease. Additionally, this exploration empowers the approval of this work by progressively thorough trial access. We hope that the vaccine's predicted model will absolutely exhibit constructive outcomes for fixing CCHFV disease.

REFERENCES

Alam, M.M., Khurshid, A., Sharif, S., Shaukat, S., Suleman, R.M., Angez, M., Zaidi, S.S.Z., 2013. Crimean-Congo hemorrhagic fever Asia-2 genotype, Pakistan. Emerging infectious diseases 19, 1017.

BEGUM, F., Wisseman Jr, C., Casals, J., 1970. TICK-BORNE VIRUSES OF WEST PAKISTAN: IV. VIRUSES SIMILAR TO, OR IDENTICAL WITH, CRIMEAN HEMORRHAGIC FEVER (CONGO-SEMUNYA), WAD MEDANI AND PAK ARGAS 461 ISOLATED FROM TICKS OF THE CHANGA MANGA FOREST, LAHORE DISTRICT, AND OF HUNZA, GILGIT AGENCY, W. PAKISTAN. American journal of epidemiology 92, 197-202.

Benson, D.A., Karsch-Mizrachi, I., Lipman, D.J., Ostell, J., Sayers, E.W., 2008. GenBank. Nucleic acids research 37, D26-D31.

Bente, D.A., Forrester, N.L., Watts, D.M., McAuley, A.J., Whitehouse, C.A., Bray, M., 2013. Crimean-Congo hemorrhagic fever: history, epidemiology, pathogenesis, clinical syndrome and genetic diversity. Antiviral research 100, 159-189.

Burney, M., Ghafoor, A., Saleen, M., Webb, P., Casals, J., 1980. Nosocomial Outbrak of Viral Hemorrhagic Fever Caused by Crimean Hemorrhagic Fever-Congo Virus in Pakistan, January 1976. The American journal of tropical medicine and hygiene 29, 941-947.

Casals, J., 1969. Antigenic similarity between the virus causing Crimean hemorrhagic fever and Congo virus. Proceedings of the Society for Experimental Biology and Medicine 131, 233-236.

Coffman, R.L., Sher, A., Seder, R.A., 2010. Vaccine adjuvants: putting innate immunity to work. Immunity 33, 492-503.

Craig, D.B., Dombkowski, A.A., 2013. Disulfide by Design 2.0: a web-based tool for disulfide engineering in proteins. BMC bioinformatics 14, 346.

Davies, M.N., Flower, D.R., 2007. Harnessing bioinformatics to discover new vaccines. Drug discovery today 12, 389-395.

DeLano, W.L., 2002. Pymol: An open-source molecular graphics tool. CCP4 Newsletter on protein crystallography 40, 82-92.

Deléage, G., 2017. ALIGNSEC: viewing protein secondary structure predictions within large multiple sequence alignments. Bioinformatics.

Dhanda, S.K., Vir, P., Raghava, G.P., 2013. Designing of interferon-gamma inducing MHC class-II binders. Biology direct 8, 30.

Dimitrov, I., Flower, D.R., Doytchinova, I., 2013. AllerTOP-a server for in silico prediction of allergens, BMC bioinformatics. BioMed Central, p. S4.

Dodds, W.J., Different Vaccine Types and Advancements.

Dowall, S.D., Carroll, M.W., Hewson, R., 2017. Development of vaccines against Crimean-Congo haemorrhagic fever virus. Vaccine 35, 6015-6023.

Doytchinova, I.A., Flower, D.R., 2007. VaxiJen: a server for prediction of protective antigens, tumour antigens and subunit vaccines. BMC bioinformatics 8, 4.

Emmerich, P., Mika, A., von Possel, R., Rackow, A., Liu, Y., Schmitz, H., Günther, S., Sherifi, K., Halili, B., Jakupi, X., 2018. Sensitive and specific detection of Crimean-Congo Hemorrhagic Fever Virus (CCHFV)—Specific IgM and IgG antibodies in human sera using recombinant CCHFV nucleoprotein as antigen in μ-capture and IgG immune complex (IC) ELISA tests. PLoS neglected tropical diseases 12, e0006366.

Ergonul, O., 2012. Crimean–Congo hemorrhagic fever virus: new outbreaks, new discoveries. Current opinion in virology 2, 215-220.

Ergönül, Ö., 2006. Crimean-Congo haemorrhagic fever. The Lancet infectious diseases 6, 203-214.

Gasteiger, E., Gattiker, A., Hoogland, C., Ivanyi, I., Appel, R.D., Bairoch, A., 2003. ExPASy: the proteomics server for in-depth protein knowledge and analysis. Nucleic acids research 31, 3784-3788.

Hall, T.A., 1999. BioEdit: a user-friendly biological sequence alignment editor and analysis program for Windows 95/98/NT, Nucleic acids symposium series. [London]: Information Retrieval Ltd., c1979-c2000., pp. 95-98.

Hawman, D.W., Feldmann, H., 2018. Recent advances in understanding Crimean–Congo hemorrhagic fever virus. F1000Research 7.

Keshtkar-Jahromi, M., Kuhn, J.H., Christova, I., Bradfute, S.B., Jahrling, P.B., Bavari, S., 2011. Crimean-Congo hemorrhagic fever: current and future prospects of vaccines and therapies. Antiviral research 90, 85-92.

Khurshid, A., Hassan, M., Alam, M.M., Aamir, U.B., Rehman, L., Sharif, S., Shaukat, S., Rana, M.S., Angez, M., Zaidi, S.S.Z., 2015. CCHF virus variants in Pakistan and Afghanistan: Emerging diversity and epidemiology. Journal of Clinical Virology 67, 25-30.

Laskowski, R.A., 2009. PDBsum new things. Nucleic acids research 37, D355-D359.

Li, K.-B., 2003. ClustalW-MPI: ClustalW analysis using distributed and parallel computing. Bioinformatics 19, 1585-1586.

Lovell, S.C., Davis, I.W., Arendall III, W.B., De Bakker, P.I., Word, J.M., Prisant, M.G., Richardson, J.S., Richardson, D.C., 2003. Structure validation by Cα geometry: ϕ, ψ and Cβ deviation. Proteins: Structure, Function, and Bioinformatics 50, 437-450.

Lundegaard, C., Lamberth, K., Harndahl, M., Buus, S., Lund, O., Nielsen, M., 2008. NetMHC-3.0: accurate web accessible predictions of human, mouse and monkey MHC class I affinities for peptides of length 8–11. Nucleic acids research 36, W509-W512.

Mild, M., Simon, M., Albert, J., Mirazimi, A., 2010. Towards an understanding of the migration of Crimean–Congo hemorrhagic fever virus. Journal of general virology 91, 199-207.

Oany, A.R., Ahmad, S.A.I., Hossain, M.U., Jyoti, T.P., 2015. Identification of highly conserved regions in L-segment of Crimean–Congo hemorrhagic fever virus and immunoinformatic prediction about potential novel vaccine. Advances and applications in bioinformatics and chemistry: AABC 8, 1.

Pandey, R.K., Bhatt, T.K., Prajapati, V.K., 2018. Novel immunoinformatics approaches to design multi-epitope subunit vaccine for malaria by investigating anopheles salivary protein. Scientific reports 8, 1-11.

Patronov, A., Doytchinova, I., 2013. T-cell epitope vaccine design by immunoinformatics. Open biology 3, 120139.

Peng, J., Xu, J., 2011. RaptorX: exploiting structure information for protein alignment by statistical inference. Proteins: Structure, Function, and Bioinformatics 79, 161-171.

Rapin, N., Lund, O., Bernaschi, M., Castiglione, F., 2010. Computational immunology meets bioinformatics: the use of prediction tools for molecular binding in the simulation of the immune system. PLoS One 5.

Saha, S., Raghava, G., 2006. Prediction of continuous B-cell epitopes in an antigen using recurrent neural network. Proteins: Structure, Function, and Bioinformatics 65, 40-48.

Saleem, M., Shah, S.Z., Haidari, A., Idrees, F., 2016. Prevalence of Crimean-Congo hemorrhagic fever in Pakistan and its new research progress. Journal of Coastal Life Medicine 4, 259-262.

Schmaljohn, C., 2001. Bunyaviridae: the viruses and their replication. Fields of Virology.

Sharp, P.M., Li, W.H., 1987. The codon Adaptation Index--a measure of directional synonymous codon usage bias, and its potential applications. Nucleic Acids Res 15, 1281-1295.

Simon, M., Johansson, C., Mirazimi, A., 2009. Crimean-Congo hemorrhagic fever virus entry and replication is clathrin-, pH-and cholesterol-dependent. Journal of General Virology 90, 210-215.

Soria-Guerra, R.E., Nieto-Gomez, R., Govea-Alonso, D.O., Rosales-Mendoza, S., 2015. An overview of bioinformatics tools for epitope prediction: implications on vaccine development. Journal of biomedical informatics 53, 405-414.

Tipu, H.N., 2016. Immunoinformatic analysis of crimean Congo hemorrhagic fever virus glycoproteins and epitope prediction for synthetic peptide vaccine. J Coll Physicians Surg Pak 26, 108-112.

Tomar, N., De, R.K., 2010. Immunoinformatics: an integrated scenario. Immunology 131, 153-168.

Tovchigrechko, A., Vakser, I.A., 2006. GRAMM-X public web server for protein–protein docking. Nucleic acids research 34, W310-W314.

Wang, P., Sidney, J., Kim, Y., Sette, A., Lund, O., Nielsen, M., Peters, B., 2010. Peptide binding predictions for HLA DR, DP and DQ molecules. BMC bioinformatics 11, 568.

Whitehouse, C.A., 2004. Crimean–Congo hemorrhagic fever. Antiviral research 64, 145-160.

Wiederstein, M., Sippl, M.J., 2007. ProSA-web: interactive web service for the recognition of errors in three-dimensional structures of proteins. Nucleic acids research 35, W407-W410.

Xu, D., Zhang, Y., 2011. Improving the physical realism and structural accuracy of protein models by a two-step atomic-level energy minimization. Biophysical journal 101, 2525-2534.

Yilmaz, R., Kundak, A.A., Ozer, S., Esmeray, H., 2009. Successful treatment of severe Crimean-Congo hemorrhagic fever with supportive measures without ribavirin and hypothermia. Journal of Clinical Virology 44, 181-182.

Zivcec, M., Safronetz, D., Scott, D.P., Robertson, S., Feldmann, H., 2018. Nucleocapsid protein-based vaccine provides protection in mice against lethal Crimean-Congo hemorrhagic fever virus challenge. PLoS neglected tropical diseases 12, e0006628.

Zivcec, M., Scholte, F.E., Spiropoulou, C.F., Spengler, J.R., Bergeron, É., 2016. Molecular insights into Crimean-Congo hemorrhagic fever virus. Viruses 8, 106.

License

Table 1: Conserved Regions among Glycoprotein and RNA Dependent RNA Polymerase

Proteins	Conserved Regions	Position
RNA dependent RNA polymerase	NFNVCKRLTGRSTGERLPRSVRSKVIYEMVKLVGETGMAI	2211-2329
	LQQLAFAQALNYEHRFYAVLAPKAQLGGARDLLVQETGT	
	KVMHATTEMFSRNLLKTTSDDGLTNPHLKETILNVGLDCL	
	NMRNLDGKPISEGSNLVNFYKVICISGDNTKWG	2331-2363
Glycoprotein	NLLNSTSLETSLSIEAPWGAINV	1056-1078
	ANIALSWSSVEHRGNKILV	1089-1107
	SWDLGVEDASESKLLTVS	1124-1141
	MDLSQMYSPVFEYLSGDRQVEEWPKATCTGDCPERCGCT	1143-1214
	SSTCLHKEWPHSRNWRCNPTWCWGVGTGCTCCG	
	YIKTEAIVCVELTSQERQCSLIEAGTRFNLGPVTITLSEPRNI	1233-1283
	QQKLPPEI	
	VLSASTVCKLQSCTHG	1303-1318
	HFNTSWMSWDGCDLDYYCNMGDWPSC	1348-1373
	FHFHSKRVTAHGDTPQLDLKARPTYGAGE	1400-1428
	TVLVEVADMELHTKK	1430-1444
	CTGCYACSSGISCKV	1457-1471
	IHVDEPDELTVHVKS	1473-1487
	PQSILIEHKGTI	1552-1563
	ILFCFKCCRRTRGL	1624-1637
	LLDGERLADR	1667-1676
	IAELFSTK	1678-1685

Table 2: CTL Epitopes Predicted by Netmhc 2.0 Server

Protein	Peptide Sequence(Position)	HLA Class I Alleles												Antigenicity
		HLA* 0101	HLA* 0201	HLA* 0301	HLA*2 402	HLA* 2601	HLA* 0702	HLA* 0801	HLA* 2705	HLA* 3901	HLA* 4001	HLA* 5801	HLA* 1501	
RNA dependent RNA polymerase	RFYAVL APK (55-63)													0.7
	KPISEGS NL (8-16)													0.7
	NPHLKE TIL (104-112)													0.8
	QQLAFA QAL (42-50)													0.4
	YEHRFY AVL (52-60)													0.6
	KETILNV GL (108-116)													0.9
	MAILQQ LAF (38-46)													0.6
	LAFAQA LNY (44-52)													0.7
	QALNYE HRF (48-56)													1.3
Glycoprotein	VSMDLS QMY													0.5
	GTGCTC CGY													0.4
	ILVSWD LGV													0.9
	KLLTVS MDL													0.4
	RLADRI AEL													0.9
	RIAELFS TK													0.6
	TEAIVCV EL													1.1
	IEAGTRF NL													1
	IEHKGTII L													0.9
	TSLSIEA PW													0.9
	NVANIA LSW													1.5
	SSTCLH KEW													0.8
	RNWRCN PTW													0.9
	HFNTSW MSW													0.9
	SLIEAGT RF													0.4

Table 3: HTL Epitopes predicted by IEDB Consensus Method

Protein	Peptide	Position	Class	Antigenicity
RNA dependent RNA polymerase	HRFYAVLAPKAQ	54-65	HLA-DRB1*01:01, HLA-DPA1*01:03/DPB1*14:01, HLA-DPA1*01:03/DPB1*05:01, HLA-DRB1*09:01, HLA-DRB3*02:02, HLA-DQA1*01:01/DQB1*04:02, HLA-DRB1*04:01, HLA-DRB1*11:01, HLA-DPA1*01:03/DPB1*01:01,	0.6
	RFYAVLAPKAQL	55-66	HLA-DRB1*01:01, HLA-DPA1*01:03/DPB1*14:01, HLA-DRB1*09:01, HLA-DPA1*01:03/DPB1*05:01, HLA-DRB3*02:02, HLA-DRB1*11:01, HLA-DQA1*01:01/DQB1*02:01	0.5
	EHRFYAVLAPKA	53-64	HLA-DPA1*01:03/DPB1*14:01, HLA-DQA1*01:01/DQB1*04:02, HLA-DRB1*01:01, HLA-DPA1*01:03/DPB1*05:01, HLA-DPA1*01:03/DPB1*01:01, HLA-DRB1*09:01, HLA-DRB3*02:02, HLA-DQA1*01:01/DQB1*06:02, HLA-DRB1*04:01	0.7
	FYAVLAPKAQLG	56-67	HLA-DRB1*01:01, HLA-DPA1*01:03/DPB1*14:01, HLA-DRB1*09:01	0.7
	YEHRFYAVLAPK	52-63	HLA-DQA1*01:01/DQB1*04:02, HLA-DPA1*01:03/DPB1*14:01, HLA-DPA1*01:03/DPB1*05:01, HLA-DPA1*01:03/DPB1*01:01	0.8
	NYEHRFYAVLAP	51-62	HLA-DQA1*01:01/DQB1*04:02	0.8
	ETGMAILQQLAF	35-46	HLA-DQA1*01:01/DQB1*06:02, HLA-DQA1*01:01/DQB1*03:02, HLA-DRB4*01:01	0.8
	GETGMAILQQLA	34-45	HLA-DQA1*01:01/DQB1*06:02, HLA-DQA1*01:01/DQB1*03:02, HLA-DQA1*01:01/DQB1*03:01	0.6
	GMAILQQLAFAQ	47-48	HLA-DRB4*01:01, HLA-DRB1*12:01	0.6
	QQLAFAQALNYE	42-53	HLA-DQA1*01:01/DQB1*03:02, HLA-DQA1*01:01/DQB1*02:01, HLA-DQA1*01:01/DQB1*06:02	0.8
	MAILQQLAFAQA	38-49	HLA-DRB4*01:01, HLA-DRB1*12:01	0.5
	VGETGMAILQQL	33-44	HLA-DQA1*01:01/DQB1*03:02, HLA-DQA1*01:01/DQB1*06:02	0.7
	LQQLAFAQALNY	41-52	HLA-DQA1*01:01/DQB1*06:02, HLA-DQA1*01:01/DQB1*04:02	0.6
	TGMAILQQLAFA	36-47	HLA-DRB4*01:01, HLA-DQA1*01:01/DQB1*06:02	0.8
Glycoprotein	TVLVEVADMELH	1-12	HLA-DQA1*01:01/DQB1*02:01	0.8
	VLVEVADMELHT	2-13	HLA-DQA1*01:01/DQB1*02:01	0.5
	NIALSWSSVEHR	2-13	HLA-DQA1*01:01/DQB1*04:02	1.7
	PVTITLSEPRNI	32-43	HLA-DRB1*13:02, HLA-DRB1*07:01	0.8
	VTITLSEPRNIQ	33-44	HLA-DRB1*07:01, HLA-DRB1*09:01, HLA-DRB1*13:02	0.8
	IKTEAIVCVELT	2-13	HLA-DQA1*01:01/DQB1*03:02	1.5
	SLETSLSIEAPW	7-18	HLA-DQA1*01:01/DQB1*03:02	0.7
	IALSWSSVEHRG	3-14	HLA-DQA1*01:01/DQB1*04:02	1.5
	LFCFKCCRRTRG	2-13	HLA-DRB1*11:01	1.3
	FCFKCCRRTRGL	3-14	HLA-DRB1*11:01	1.6
	FHFHSKRVTAHG	1-12	HLA-DRB1*11:01	0.8
	ANIALSWSSVEH	1-12	HLA-DQA1*01:01/DQB1*04:02, HLA-DQA1*01:01/DQB1*03:02, HLA-DQA1*01:01/DQB1*06:02	1.3
	RFNLGPVTITLS	27-38	HLA-DRB1*01:01	2.0

Table 4: Linear B Cell Epitopes Predicted through ABCPred 2.0 Server

Protein	B-Cell Epitopes (Positions)	Antigenicity
RNA dependent RNA polymerase	LNVGLDCLNMRNLD(112)	2.2164
	NPHLKETILNVGLD(104)	0.9591
	LQQLAFAQALNYEH(41)	0.8395
	MRNLDGKPISEGSN(121)	0.5817
	SDDGLTNPHLKETI(98)	0.4297
	YAVLAPKAQLGGAR(57)	0.5983
	QALNYEHRFYAVLA(48)	1.0345
	ETGMAILQQLAFAQ(35)	0.7284
Glycoprotein	NWRCNPTWCWGVGT(113)	1.2279
	SLSIEAPWGAINVA(113)	0.9670
	GNKILVSWDLGVED(37)	0.4731
	TAHGDTPQLDLKAR(234)	0.6251
	YCNMGDWPSCFHFH(216)	0.7863
	NIQQKLPPEIVLSA(174)	0.7328
	PEIVLSASTVCKLQ(181)	0.4536
	GTGCTCCGYIKTEA(125)	0.6467
	GAGETVLVEVADME(251)	0.5597
	GYIKTEAIVCVELT(132)	1.3066
	CYACSSGISCKVIH(273)	0.7572
	GAINVANIALSWSS(19)	1.2463
	QERQCSLIEAGTRF(147)	0.8540
	IALSWSSVEHRGNK(26)	1.1516
	VCVELTSQERQCSL(140)	1.4815
	TSLETSLSIEAPWG(6)	0.7585
	LDLKARPTYGAGET(242)	1.3598
	FNLGPVTITLSEPR(160)	1.6120
	WCWGVGTGCTCCGY(120)	1.1455
	SWDGCDLDYYCNMG(207)	0.6276
	EVADMELHTKKCTG(259)	0.4544
	EAGTRFNLGPVTIT(155)	1.6746
	PSCFHFHSKRVTAH(223)	1.0486

Table 5: Linear B-Cell Epitopes Identification Through Discotop Server

Residues Position	Residues Names	Number of Contacts	Propensity Score	DicsoTope Score
115	TYR	5	-3.194	-3.401
118	ARG	5	-2.473	-2.763
119	PHE	8	- 3.135	-3.694
120	ALA	0	- 3.115	-2.757
123	ASN	2	- 2.328	-2.291
124	PRO	2	- 2.334	-2.295
125	HIS	0	-2.034	-1.800
128	GLU	4	-3.043	-3.153
142	LEU	5	-3.516	-3.687
144	PRO	8	0.259	-0.691
145	GLY	8	-1.130	-1.920
146	PRO	4	-2.155	-2.368
161	PRO	0	-3.186	-2.820
177	GLY	8	-3.018	-3.591
178	PRO	0	-1.623	-1.436
179	GLY	2	-1.805	-1.828
192	ARG	4	-0.575	-0.969
193	GLY	4	0.958	0.387
194	GLY	3	0.138	-0.223
195	PRO	10	-0.845	-1.898
196	GLY	2	1.214	0.845
197	PRO	4	-1.554	-1.835

Table 6: Linear B Cell Epitopes in the Final MESV Construct

B Cell Epitope (Position)	Antigenicity
TSLSIEAPWGPGPG (168)	0.7
TRGRKCCRRKKEAA (35)	1.0
AAYNPHLKETILAA (120)	0.7
HLKETILAAYKETI (125)	0.6
IGKCSTRGRKCCRR (30)	1.2
PGSLETSLSIEAPW (163)	0.6
IVCVELTGPGPGSL (153)	0.7
LPKEEQIGKCSTRG (24)	0.7
CCRRKKEAAAKTEA (40)	0.8
NYAAYQALNYEHRF (94)	1.0
LSWSSVEHRGGPGP (184)	1.4
KETINVGLGPGPGI (135)	0.9
GMAILQQLAFGPGP (201)	1.0
YEHRFAAYNPHLKE (115)	0.7
VGLGPGPGIKTEAI (140)	1.1
GPGPGETGMAILQQ (194)	0.6
LAAYLAFAQALNYA (83)	0.6
LAFAAYQQLAFAQA (69)	0.9
AAYQALNYEHRFAA (108)	1.0
AAKTEAIVCVELAA (48)	1.0
LAFAQALAAYLAFA (77)	0.6
ILAAYKETINVGLG (130)	1.1
LNYEHRFAAYQALN (101)	0.9
PGTGMAILQQLAFA (214)	0.5

Figure Legends

Figure 1: vaccine construct. MESV vaccine sequence has 278 amino acid sequence length consisting of an adjuvant (color) linked at N terminal of MESV vaccine sequence through EAAAK linker (Color). AAY linker (color) used for joining the CTL epitopes and GPGPG linker (color) used to joined the HTL epitopes.

Figure 2: 3D structure prediction and validation of MESV vaccine construct: (A) MESV vaccine's 3D structure. (B) MEP Vaccine's refined structure. (C) PROSA validation of 3D MESV construct. (D) Ramachandran plot analysis of predicted structure

Figure 3: (A) Specific sites of B cells predicted linear epitopes on the 3D structure of vaccine (B) Specific sites of B cells discontinues epitopes predicted through DISCOTOPE 2.0 server on the 3D structure vaccine

Figure 4: Disulfide engineering to improve protein stability. Showing total 2 mutated residues pairs in magenta and gray color. These residues were selected based on their energy, chi3 value, and B-factor.

Figure 5: MESV construct docked with human TLR3: (**A**) MEV-TLR3 docked complex in cartoon representation. TLR3 displayed with purple color and MESV vaccine construct displayed with red color. All interacting residues of MEV and TLR3. 1 Hydrogen bond is shown with blue color line. The colors of interacting residues are representing properties of amino acids (Positive: Blue, Negative: Red, Neutral: Green, Aliphatic: Grey, Aromatic: Pink, Pro & Gly: Orange and Cys: Yellow)

Figure 6: Molecular dynamics simulation of the MESV-TLR3 complex, showing **a** eigenvalue; **b** deformability; **c** B-factor; **d** covariance matrix; and **e** elastic network analysis.

Figure 7: In silico immune response using MESV as antigen. (A) The antibodies, and (B) cytokines and interleukins.

Figure 8: In silico cloning of codon optimized MESV into *E. coli* K12 expression system. The plasmid back-bone is kept in black color while the inserted DNA sequence is shown in green color.